AIP | Applied Physics Letters

Radiation tolerance characterization of dual band InAs/GaSb type-II strain-layer superlattice pBp detectors using 63 MeV protons

V. M. Cowan, C. P. Morath, J. E. Hubbs, S. Myers, E. Plis et al.

Citation: Appl. Phys. Lett. **101**, 251108 (2012); doi: 10.1063/1.4772543
View online: http://dx.doi.org/10.1063/1.4772543
View Table of Contents: http://apl.aip.org/resource/1/APPLAB/v101/i25
Published by the American Institute of Physics.

Report Documentation Page

Form Approved
OMB No. 0704-0188

1. REPORT DATE	2. REPORT TYPE	3. DATES COVERED
19 DEC 2012		**00-00-2012 to 00-00-2012**

4. TITLE AND SUBTITLE	5a. CONTRACT NUMBER
Radiation tolerance characterization of dual band InAs/GaSb type-II strain-layer superlattice pBp detectors using 63 MeV protons	5b. GRANT NUMBER
	5c. PROGRAM ELEMENT NUMBER
6. AUTHOR(S)	5d. PROJECT NUMBER
	5e. TASK NUMBER
	5f. WORK UNIT NUMBER
7. PERFORMING ORGANIZATION NAME(S) AND ADDRESS(ES) **University of New Mexico,Center for High Technology Materials,Department of Electrical and Computer Engineering,Albuquerque,NM,87106**	8. PERFORMING ORGANIZATION REPORT NUMBER
9. SPONSORING/MONITORING AGENCY NAME(S) AND ADDRESS(ES)	10. SPONSOR/MONITOR'S ACRONYM(S)
	11. SPONSOR/MONITOR'S REPORT NUMBER(S)

12. DISTRIBUTION/AVAILABILITY STATEMENT
Approved for public release; distribution unlimited

13. SUPPLEMENTARY NOTES

14. ABSTRACT

15. SUBJECT TERMS

16. SECURITY CLASSIFICATION OF:			17. LIMITATION OF ABSTRACT	18. NUMBER OF PAGES	19a. NAME OF RESPONSIBLE PERSON
a. REPORT	b. ABSTRACT	c. THIS PAGE			
unclassified	**unclassified**	**unclassified**	**Same as Report (SAR)**	**5**	

Radiation tolerance characterization of dual band InAs/GaSb type-II strain-layer superlattice pBp detectors using 63 MeV protons

V. M. Cowan,[1,a)] C. P. Morath,[1] J. E. Hubbs,[1] S. Myers,[2] E. Plis,[2] and S. Krishna[2]
[1]*Air Force Research Laboratory, Space Vehicles Directorate, 3550 Aberdeen Ave. SE, Kirtland AFB, New Mexico 87117, USA*
[2]*Center for High Technology Materials, Department of Electrical and Computer Engineering, University of New Mexico, Albuquerque, New Mexico 87106, USA*

(Received 14 August 2012; accepted 3 December 2012; published online 19 December 2012)

The radiation tolerance characterization of dual band InAs/GaSb type-II strain-layer superlattice pBp detectors of varying size using 63 MeV proton irradiation is presented. The detectors' mid-wave infrared performance degraded with increasing proton fluence Φ_P up to $3.75 \times 10^{12}\,\mathrm{cm}^{-2}$ or, equivalently, a total ionizing dose = 500 kRad (Si). At this Φ_P, an ~31% drop in quantum efficiency η, ~2 order increase in dark current density J_D, and consequently, >1 order drop in calculated detectivity D^* were observed. Proton damage factors were determined for η and D^*. Arrhenius-analysis of temperature-dependent J_D measurements reflected significant changes in the activation energies following irradiation. © *2012 American Institute of Physics*. [http://dx.doi.org/10.1063/1.4772543]

Infrared (IR) hybrid detector arrays operated in the space environment may be subjected to a variety of radiation sources while in orbit. This means IR detectors intended for applications such as space-based surveillance or space-situational awareness must not only have high performance (high η and low J_D) but also their *radiation tolerance* or ability to withstand the effects of the radiation they would expect to encounter in a given orbit must be characterized. As the effects of proton interactions with hybrid detector arrays tend to dominate in space,[1] a specific detector's radiation tolerance is typically characterized by measuring its performance degradation as a function of proton irradiation fluence up to a total ionizing dose (TID) of 300 kRad(Si), which is 2–3× the maximum expected on-orbit TID value for typical surveillance applications. Radiation tolerance characterization also typically includes determining the rate of performance degradation via a damage factor analysis and, finally, temperature-dependent measurements of J_D, which are used to determine the dark current limiting mechanism via an Arrhenius-analysis and the degree to which any thermal annealing of the irradiation induced defects may occur.

Here, the results of a radiation tolerance characterization of dual band InAs/GaSb type II strained layer superlattice (T2SLS) pBp detectors of varying size, which were previously described in Ref. 2, using 63 MeV protons are reported. III-V-based detectors, such as these, are now being considered for space applications due to their relative advantage in manufacturability, compared with conventional mercury-cadmium-telluride (MCT) IR detectors, particularly in the long-wave infrared (LWIR).[3] T2SLS detectors are also theoretically predicted to have lower Auger-limited dark currents compared with MCT,[4,5] the incumbent technology for high performance space applications. However, this advantage is yet to be realized due to the lack of reliable passivation schemes and relatively higher bulk defect densities in these materials, which lead to surface- and Shockley-Read-Hall (SRH)-limited dark currents, respectively. Unipolar-barrier architecture detectors, including the pBp-detectors reported here, were recently introduced in an effort to mitigate these dark current limiting mechanisms.[6–8] By deliberate choices of the growth materials and wafer structure, the potential barriers in these detectors appear only in either the conduction or valence band to block the majority-carrier bulk and surface currents (e.g., in a pBp detector, the potential barrier appears only in the valence band). Simultaneously, the barrier layer ideally limits the depletion by an external bias to itself so the absorbing layer remains in the flatband condition, which eliminates GR-currents from whatever defects may be present in the absorbing layer.

Subjecting IR detectors to proton irradiation is expected to lead to both TID and displacement damage effects, both of which occur on orbit. TID effects occur as incoming protons lose their kinetic energy to ionization of the detector material's constituent atoms and the additional charges become trapped in oxide layers or surface traps. This additional charging may result in flat-band voltage shifts and increased surface leakage currents. TID effects generally are more visible at lower device temperatures, where charges generated in oxide layers are less mobile, and tend to anneal out at higher temperatures. Displacement damage effects result from the occasional non-ionizing energy loss of an incoming proton due to elastic or inelastic scattering with an atomic nucleus that is sufficient to knock the atom from its lattice site and generate vacancy-interstitial pair, anti-sites, and defect complexes.[9] These defects may manifest in lower η, due to the consequent reduction in minority carrier lifetime τ, and higher J_D, due to the SRH mechanism. The proton fluence at 63 MeV required to alter the background doping levels, such that the fundamental Auger mechanism is enhanced, is expected to be order's higher than the fluence levels used here. Thus, the first step to characterizing a detector's radiation tolerance is measuring η and J_D as a function of Φ_P, with all irradiation and measurements conducted at the detector's expected operating temperature and bias. The importance of the latter is vividly illustrated by

a)Author to whom correspondence should be addressed. Electronic mail: vincent.cowan@kirtland.af.mil.

recent preliminary 1–2 MeV proton irradiation studies of Sb-based T2SLS photodiodes where the detectors were unbiased and at 300 K during irradiation, which presumably precluded observing the effects of ionization and lower energy defects due to displacement damage, both of which were expected to anneal at room tempereature.[10,11] Thermal annealing of radiation effects at 300 K was shown in Ref. 1 and was likewise observed during this experiment on the T2SLS detectors. Using η and J_D to also estimate the detector sensitivity, expressed here in this letter by shot-noise-limited D^*, is then done to illustrate which of the two dominates the change in overall performance.

Radiation tolerance can be further characterized by calculating the *damage factor* K_X or the rate of degradation for each performance metric X (e.g., $X = \eta, J_D, D^*$, etc.) from the performance measurements taken versus fluence. For comparison purposes, however, it is worth noting that these K_X-metrics may be a function of a detector's architecture, material composition, growth method, processing, passivation, etc., and are thus entirely specific to that particular detector. K_X's are also specific to the particle type and energy of the irradiation. In fact, with a known energy-dependence $K_X(E)$ predictions of the expected on-orbit degradation ΔX ideally become possible, according to $\Delta X = \int_{E_1}^{E_2} K_X(E) \frac{d\Phi_P}{dE} dE$, where $\frac{d\Phi_P}{dE}$ is an expected orbit's differential proton fluence spectrum.[1]

Temperature-dependent measurements of J_D at the expected operating bias are also used to characterize the effects of proton irradiation on IR detectors. Determining the activation energy, E_A, via an Arrhenius-type analysis of the J_D-measurements allows for changes in the limiting mechanism of J_D at specific temperatures to be discerned if it is done prior to and immediately following irradiation. These are henceforth referred to as the *pre-rad* and *post-rad* conditions, respectively. As the post-rad detector is warmed up to room temperature, it is also often the case that some degree of thermal annealing of the irradiation induced defects will occur. Thus, a third set of temperature-dependent J_D-measurements is typically performed after this initial warm-up, henceforth referred to as the *post-anneal* condition, to characterize the effects of any thermal annealing. A standard η and J_D-measurement at the expected operating conditions are also usually performed post-anneal.

The dual-band, InAs/GaSb T2SLS pBp detectors used in this study were previously fully described in Ref. 2. Summarizing those details, the pBp detectors are grown via molecular beam epitaxy on GaSb substrate material and include two 2 μm, p-type, Be-doped $\sim 1 \times 10^{16}\,\mathrm{cm}^{-3}$, InAs/GaSb SLS absorbing layers designed for mid-wave infrared (MWIR) and LWIR response that are separated by a similarly doped InAs/AlSb barrier layer. Samples with square mesa devices varying in mesa edge length L from 45 to 145 μm and etched through both absorber layers to the bottom contact layer were then fabricated from the material by standard photolithography and wet-etching practices and then wirebonded to 68 pin leadless chip carriers for cryogenic testing purposes. FTIR absorption measurements at forward- and reverse-bias showed the zero-response cutoff wavelength λ_c in the MWIR and LWIR were 7.8 and 12 μm at 80 K, respectively. However, only the MWIR optical results are discussed in this letter as the low LWIR signal level prevented a completely reliable radiation tolerance characterization for that band.

The proton irradiation was performed at the Crocker Nuclear Laboratory at the University of California, Davis, using their 76″ isochronous cyclotron, which can provide protons with energies up to 68 MeV.[12] The detectors were at their nominal operating conditions, biased at $V_B = +0.1$ V and $T = 80$ K, during proton irradiation. Photocurrent and dark current measurements were performed on $L = 45$, 65, 85, and 145 μm mesa devices at TID = 0, 2, 5, 10, 20, 50, 100, 200, and 500 kRad(Si), as well as following a post-rad, 2 day, 300 K thermal anneal.

Photocurrent measurements were taken with the detectors held at the MWIR operating bias, $V_B = +0.1$ V applied to the top of each mesa, using standard ac lock-in technique at $f/\# \sim 40$ and a blackbody source at $T_{BB} = 900$ K. The blackbody output was passed through a room-temperature 3.5–4.2 μm IR band-pass filter and a KRS5 dewar window, followed by a 4 mm pinhole held at 77 K within the dewar, leading to an incident photon flux $E_Q = 3.1 \times 10^{14}$ ph/s-cm^2 at peak wavelength $\lambda_p \sim 3.9$ μm. For mesa detectors, the photocurrent is given by $I_p = q\eta E_Q L^2$, where q is the charge of an electron. Thus, $\sqrt{I_p}$ was plotted as a function of L and a weighted, least squares linear fitting was performed. The fitting's slope parameter m was then used to determine η according to the expression $\eta = m^2/qE_Q$.

Dark current measurements were then performed using a standard dc source-measurement unit with a 77 K shutter blocking the pinhole. As it is typically more sensitive to irradiation, dark current was always measured following the I_{photo} measurements, to allow for any transient effects to fully diminish. Finally, temperature-dependent measurements of J_D were performed from $T = 77$ K to 300 K at the MWIR operating bias $V_B = +0.1$ V and an Arrhenius-analysis was performed to determine E_A and thus, gain some insight regarding the dark current limiting mechanism.

Measurements of the detector's η at $\lambda_p \sim 3.9$ μm, derived from the I_p-measurements, as function of Φ_P and post-anneal are shown in Fig. 1. In the pre-rad condition, as Fig. 1 shows,

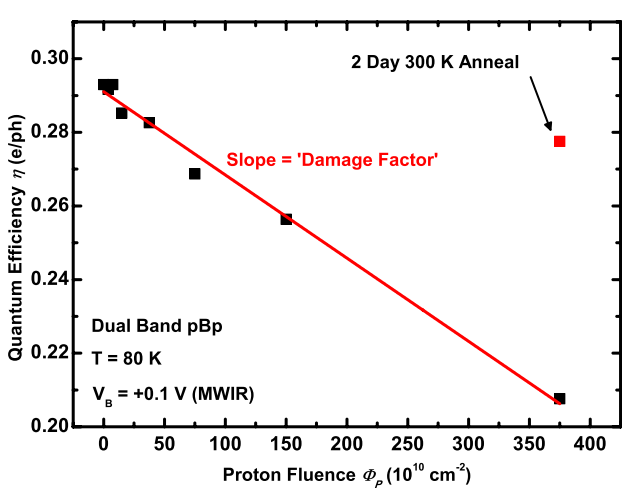

FIG. 1. η at $\lambda_p \sim 3.9$ μm plotted as a function of Φ_P ranging from 0 to $3.75 \times 10^{12}\,\mathrm{cm}^{-2}$ and post-anneal. A $K_\eta = -2.26 \times 10^{-14}$ e-cm^2/ph-H$^+$ was calculated from the linear fitting of the measured data.

$\eta \sim 29\%$, which roughly matches the result given in Ref. 10. The η was then observed to degrade roughly linearly with increasing Φ_P down to ~21% at $3.75 \times 10^{12}\,\mathrm{cm}^{-2}$ or, equivalently, TID = 500 kRad(Si), a 28% change in η. From the slope of the data in Fig. 1, the MWIR η damage factor was found to be $K_\eta = -2.14 \times 10^{-14}$ e-cm^2/ph-H$^+$. Following irradiation, the detector temperature was raised to 290 K for ~ 48 h and then re-measured, whereby η recovered to ~28%. As proton irradiation is known to generate bulk defects, and thereby reduce τ and diffusion length $L_D \propto \sqrt{\tau}$, the drop in η in Fig. 1 suggests $\eta \propto 1 - e^{-\alpha L_D}$, where α is the absorption coefficient and $L_D < 2\,\mu$m, the thickness of the MWIR absorbing layer, since α is not expected to change with fluence. A perimeter-to-area (P/A) analysis of these results, which suggests some surface-related recombination is also occurring, will be discussed in a forthcoming publication.[13]

Measurements of J_D at $V_B = +0.1$ V as a function of Φ_P and post-anneal for each detector are shown in Fig. 2, while the inset shows the measured I-V relationship for the 45 μm device under similar conditions. These results all show a monotonic increase in J_D with increasing Φ_P, up to $3.75 \times 10^{12}\,\mathrm{cm}^{-2}$, at which point a roughly two order increase in J_D was observed. For $\Phi_P < 10^{12}\,\mathrm{cm}^{-2}$, however, the rate of increase of J_D appears to depend on L, which is indicative of surface currents. A perimeter-to-area analysis of J_D to investigate the surface current effect will also be discussed in the other forthcoming publication.[13] For $\Phi_P > 10^{12}\,\mathrm{cm}^{-2}$, the change in J_D appears to saturate slightly; however, this effect requires more investigation and may be transient. Following irradiation, two consecutive thermal anneals, at 240 K for 2 h and at 300 K for 48 h, were conducted. Following each an ~25% and ~50% reduction in irradiation induced J_D were observed.

To approximate the expected reduction in sensitivity with increasing Φ_P, the shot-noise limited D^* for the 45 μm detector was then calculated from the results in Figs. 1 and 2 using the expression $D^* = R \Big/ \sqrt{\left(2qJ + (4k_BT)/R_dA_d\right)}$, where $R = \eta q/(hc/\lambda_p)$ is the detector responsivity, k_B is Boltzmann's constant, R_d is differential resistance, A_d is the detector area, h is Planck's constant, and c is the speed of light. While this method of calculating D^* is often of limited utility in accurately describing the detector's sensitivity, due to the omission of additional noise sources as described in Ref. 14, as it is used here it serves as a good means of estimating the sensitivity's dependence on Φ_P. A plot of D^*, again as function of Φ_P and post-anneal, is given in Fig. 3. Here, D^* is predicted to degrade over an order of magnitude from its pre-rad value of 4.86×10^{10} cm Hz$^{1/2}$/W down to 2.12×10^{9} cm Hz$^{1/2}$/W in post-rad. Fig. 3 also includes plots of D^* calculated with either η or J_D held fixed at its pre-rad value. These two plots show that the dependence of D^* on Φ_P is completely dominated by changes in J_D. Post-anneal, only a 49% drop in D^* is calculated compared to the pre-rad condition. For $\Phi_P < 100 \times 10^{10}\,\mathrm{cm}^{-2}$, a D^* damage factor $K_{D^*} \sim 4.53 \times 10^{-2}$ cm^3-Hz$^{1/2}$/W-H$^+$ was determined.

Three sets of temperature-dependent J_D-measurements, reflecting the pre-rad, post-rad, and post-anneal conditions, for the 45 μm mesa detector at $V_B = +0.1$ V are shown in Fig. 4. Here, the pre-rad and post-anneal results clearly show two distinct regions of T-dependence, with crossovers at $T = 115$ K and 93 K, respectively, while for the post-rad data this is much less clear. From the Arrhenius-analysis of the pre-rad and post-anneal plots in Fig. 4, an $E_A \sim 155$ meV was extracted for the high-T region, which directly corresponds to the measured $\lambda_c \sim 8.1\,\mu$m for this device and indicates diffusion-limited J_D in this region. In the low-T region, slightly different $E_A < E_{gap}/2$ and amplitudes were determined for the pre-rad and post-anneal data. These differences suggest J_D is SRH-limited with additional irradiation-induced defects that remained non-annealed affecting the post-anneal data. The post-rad J_D data had an E_A as low as 20 meV up to $T \sim 115$ K and slowly increasing until $T \sim 175$ K, when it begins to show a similar high-T dependence as the other traces, presumably due to the combined effects of thermal annealing and enhancement of the diffusion-limited J_D with T. The low E_A and high amplitude for the post-rad J_D at $T < 175$ K, in comparison with the other traces, most likely reflects surface-limited behavior

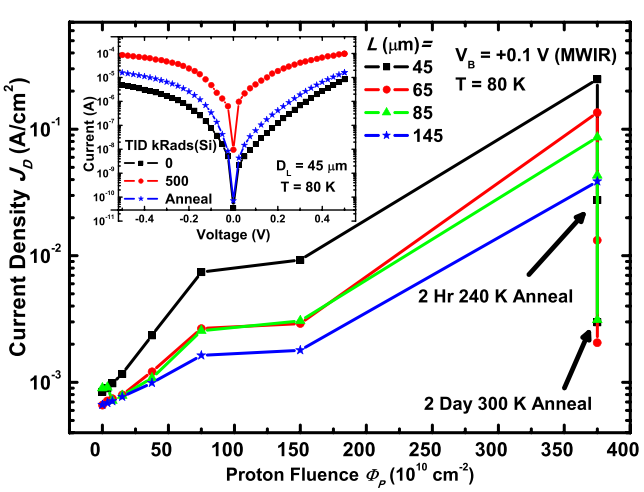

FIG. 2. J_D measured for the $L = 45$, 65, 85, and 145 μm detectors at Φ_P ranging from 0 to $3.75 \times 10^{12}\,\mathrm{cm}^{-2}$ and post-anneal. Inset: I-V relationship for 45 μm detector in pre-rad, post-rad, and post-anneal conditions.

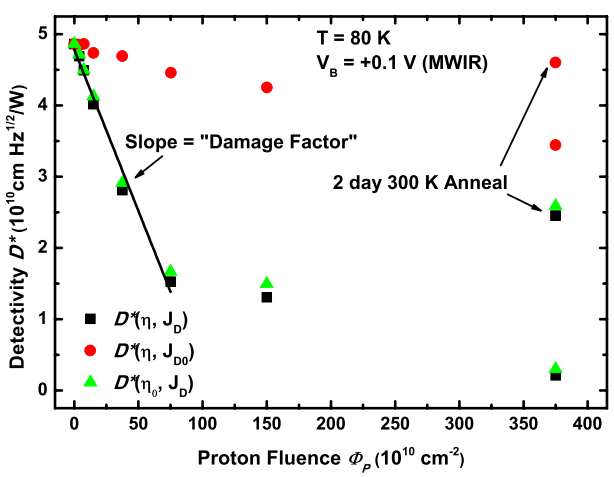

FIG. 3. Shot-noise limited D^* (black squares) for 45 μm mesa detector with Φ_P ranging from 0 to $3.75 \times 10^{12}\,\mathrm{cm}^{-2}$ and post-anneal and with η (red circles) and J_D (green triangles) fixed to its pre-rad values. The linear fitting had a slope of $K_{D^*} \sim 4.53 \times 10^{-2}$ (cm^3 Hz$^{1/2}$/W H$^+$).

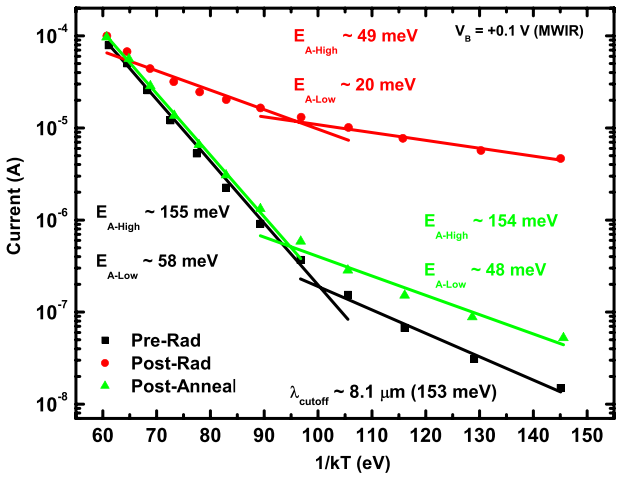

FIG. 4. Temperature-dependent J_D measurements on the 45 μm detector in the pre-rad, post-rad, and post-anneal conditions illustrating changes in E_A that reflect an increase (decrease) in near mid-gap defect density post-rad (post-anneal).

stemming from TID effects as the dark current nearly recovers to its pre-rad value following the 300 K thermal anneal.

In conclusion, a radiation tolerance characterization of a pBp detector employing a T2SLS absorber was performed using 63 MeV proton irradiation. Measurements of η and J_D reflected a degradation of the detector performance with increasing Φ_P that would necessarily result in >1 order drop in the calculated D^* at $\Phi_P = 3.75 \times 10^{12}\,\mathrm{cm}^{-2}$, mostly from the increase of J_D with Φ_P. Post-anneal, both η and J_D recovered to a large degree to their near pre-rad values. An Arrhenius-analysis of temperature-dependent J_D-measurements reflected significant changes in E_A and amplitudes following irradiation, which suggested a large increase in the surface current, most of which recovered following a 48 h, 300 K thermal anneal, and a smaller increase in bulk dark current, which did not anneal out, following irradiation.

This work was partially supported by AFOSR FA9550-10-1-0113 and AFRL FA9453-12-1-0336.

[1]J. E. Hubbs P. W. Marshall, C. J. Marshall, M. E. Gramer. D. Maestas, J. P. Garcia, G. A. Dole, and A. A. Anderson, IEEE Trans. Nucl. Sci. **54**(6), 2435 (2007).
[2]E. A. Plis, S. S. Krishna, N. Gautam, S. Myers, and S. Krishna, IEEE Photonics J. **3**, 234–240 (2011).
[3]A. Rogalski, Rep. Prog. Phys. **68**(10), 2267–2336 (2005).
[4]C. Grein, P. M. Young, M. E. Flatte, and H. Ehrenreich, J. Appl. Phys. **78**, 7143 (1995).
[5]D. L. Smith and C. Maihiot, J. Appl. Phys. **62**, 2545 (1987).
[6]S. Maimon and G. W. Wicks, Appl. Phys. Lett. **89**, 151109 (2006).
[7]E. H. Aifer, J. G. Tischler, J. H. Warner, I. Vurgaftmen, W. W. Bewley, J. R. Meyer, J. C. Kim, L. J. Whitman, C. I. Canedy, and E. M. Jackson, Appl. Phys. Lett. **89**, 053519 (2006).
[8]B. M. Nguyen, S. Bogdanov, S. A. Pour, and M. Razeghi, Appl. Phys. Lett. **95**(18), 183502 (2009).
[9]C. Claeys and E. Simoen, *Radiation Effects in Advanced Semiconductor Materials and Devices* (Springer, New York, 2002), pp. 9–35.
[10]B. D. Weaver and E. H. Aifer, IEEE Trans. Nucl. Sci. **56**, 3307–3309 (2009).
[11]E. M. Jackson, E. H. Aifer, C. L. Canedy, J. A. Nolde, C. D. Cress, B. D. Weaver, I. Vurgaftman, J. Warner. J. R. Meyer, J. G. Tishchler, S. A. Shar, and C. R. Dedianous, J. Electron. Mater. **39**(7), 852 (2010).
[12]C. M. Castaneda, in Proceedings of the IEEE Radiation Effects Data Workshop (2001), pp. 77–81.
[13]V. M. Cowan and C. P. Morath, "Bulk and surface current modification by proton irradiation in dual band pBp infrared detectors" (unpublished).
[14]V. M. Cowan, C. P. Morath, S. Myers, N. Gautam, and S. Krishna, Proc. SPIE **8012**, 801210 (2011).